Fibroblasts regulate lymphatic barrier functions in a tissue dependent manner

Sarfaraz Ahmad Ejazi[1], Aisha Abdulkarimu[1], Theodore Hsiao[1], Rony Garcia-Vivas[1], Katharina Maisel[1*]

Affiliations:

1: Fischell Department of Bioengineering, University of Maryland, College Park

*** Correspondence to:**

Dr. Katharina Maisel

Fischell Department of Bioengineering

University of Maryland, College Park

Email: maiselka@umd.edu

ABSTRACT

The lymphatic vasculature plays a vital role in clearing interstitial fluid and antigens from tissues and guiding immune cell migration. Junctions between lymphatic endothelial cells (LECs) are important for preserving vascular integrity and permitting transport or migration into the vessel. Tight junction proteins, like ZO-1, work alongside adherens junction proteins, like VE-cadherin, to regulate lymphatic barrier function and permeability. Fibroblasts contribute to the lymphatic interstitial environment by producing extracellular matrix and producing growth factors that induce lymphangiogenesis. Despite their known roles, the direct impact of fibroblasts on LEC barrier functions, specifically permeability and cell-cell junctions, as well as the underlying mechanisms remains poorly understood. Here, we established a non-contact in vitro co-culture system to investigate how fibroblasts affect LEC junctions and permeability. We determined the effect of secreted factors (secretomes) from normal human dermal fibroblasts (NHDFs) on human LECs (hLECs) and found that these led to a >120% increase in the transendothelial electrical resistance (TEER) of hLEC monolayer. Immunofluorescence analysis revealed a >4-fold increase in the expression of ZO-1 and VE-cadherin, and a 24% reduction in transport of FITC- dextran upon NHDF secretome treatment. Co-culture of hLECs with NHDFs also more than doubled TEER, and increased ZO-1 and VE-cadherin expression by 1.3-1.6 and 2-fold, respectively, compared

to untreated controls. Dextran permeability dropped by 15-30% after NHDF treatment. Finally, we found a significant increase in the continuity of ZO-1 junctions in hLECs co-cultured with NHDFs. Surprisingly, we found an opposite effects on hLEC junctional integrity and permeability with normal human lung fibroblast (NHLF) secretomes: NHLFs significantly lowered TEER along with ZO-1 expression and doubled dextran permeability across hLECs. Finally, we found that treatment of hLECs with thrombin, a potent inflammatory mediator, led to impaired cell junctions and increased transport only in the presence of NHDFs. This study highlights the role of fibroblasts in regulating lymphatic barrier function by modulating endothelial cell-cell junctions. Notably, their impact on LECs varies based on the tissue origin, revealing functional heterogeneity. Our findings offer valuable insights and novel therapeutic targets for modulating lymphatic functions in disease and provide foundations for strategies to improve lymphatic targeted drug delivery.

INTRODUCTION

Lymphatic vessels are found throughout the entire body and are responsible for transporting immune cells, regulating fluid homeostasis, and absorbing dietary fats. Dysfunction of the lymphatic vasculature can contribute to a range of pathological conditions, including lymphedema, chronic inflammation, and cancer progression. Lymphatic vessels are lined with lymphatic endothelial cells (LECs) with distinct morphological and functional arrangements. The initial (or capillary) lymphatics are lined with LECs, loosely connected with discontinuous (button-like) junctions and a discontinuous basement membrane with no perivascular cells. Fluid, antigens, cells, and debris are transported into initial lymphatics from the peripheral tissues and upon collection into to the initial vessel lumen, the lymph fluid is shuttled into pre-collectors and eventually larger collecting vessels. Collecting lymphatics are lined with LECs connected with continuous, tight (zipper-like junctions) cell-cell junctions and have a complete basement membrane surrounded by smooth muscle cells (SMCs) and perivascular cells. The paired leaflet valves and phasic contraction of SMCs facilitate the directional lymph flow in the collecting lymphatics and toward the thoracic ducts.

Two junction types, tight and adherens junctions, regulate lymphatic integrity and permeability, and are arranged in either button or zipper like fashion in initial and collecting vessels, respectively. Studies have highlighted the role of adherens junction proteins, including VE-cadherin, in supporting button-like junctions of initial lymphatics. A decrease in VE-cadherin expression may enhance lymphatic vessel permeability and allow immune cells to migrate into lymphatic vessels [1,2]. Tight junction proteins such as claudin-5 and zonula occludins (ZO) regulate paracellular permeability by forming an inter-cellular barrier to control the movement of proteins, molecules, and ions across the LECs. ZO-1 interacts with tight junction proteins and actin filaments to maintain LEC junctional integrity. Expression of claudin-5 and ZO-1 was found to be downregulated in inflammation, suggesting changes in lymphatic vessel permeability [3]. Alterations in expression or function of these proteins have been linked to several pathological conditions related to lymphatic dysfunction, including edema, inflammation, and cancer metastasis [4]. Indeed, many factors including inflammatory cytokines, vascular endothelial growth factor (VEGF-C), and mechanical forces like fluid shear stress and interstitial pressure, can affect the integrity of LEC junctions and lymphatic vessel permeability [5-7]

Advancements in lymphatic vascular biology revealed the complex interplay between LECs and other cell types, and researchers have attempted to identify cells and molecular signals that affect lymphatic permeability [8]. In the interstitium, lymphatic vessels are surrounded by various

extracellular matrix (ECM) proteins and residing immune cells and fibroblasts. Fibroblasts secrete ECM proteins such as collagen and can directly modulate the mechanical environment adjacent to lymphatic vessels. Fibroblasts have also been shown to secrete VEGF-C, which is known to regulate lymphangiogenesis by promoting vascular sprouting, tube formation, and vessel integrity through stimulating VEGFR3-mediated MAPK/ERK and AKT intracellular pathways [9-12]. The role of fibroblast growth factor (FGF) signaling in lymphangiogenesis was also demonstrated, as vessel sprouting was inhibited following the knockdown of FGFR1 in dermal LECs [13].

In the context of lymphatic vessels, fibroblasts have been studied in several physiological and pathological conditions, such as cancer and wound healing. For example, cancer-associated fibroblasts contribute to metastasis by inducing lymphangiogenesis and promoting lymphatic permeability within the tumor microenvironment by downregulating VE-cadherin [14]. Additionally, tumor-derived fibroblasts from head and neck cancer increased in lymphatic vessel sprouting and altered in lymphatic permeability [15]. Fibroblasts have also been implicated in the repair and regeneration of lymphatic vessels during wound healing. An in vitro engineered lymphatic model demonstrated fibroblast matrix guided lymphangiogenesis in wound healing [16].

To investigate the complex crosstalk of lymphatic endothelial cells in appropriate matrix and living fibroblasts, a co-culture system has been utilized in many studies. Most of the recent studies on the influence of LECs in response to fibroblasts have focused on lymphangiogenesis or immune and cancer cell trafficking, mainly in the context of disease. However, the homeostatic effects of fibroblast cells on lymphatic barrier function and integrity are not well understood. Here, we developed a non-contact in vitro co-culture model to examine fibroblasts regulation of lymphatic cell-cell junctions, barrier integrity, and permeability. We first studied the response of human LECs (hLECs) to secreted factors from normal human dermal fibroblasts (NHDFs) on LEC junction integrity and permeability and found a tissue-specific differences. We further studied fibroblasts/LEC co-cultures on collagen beds, where NHDFs appeared to support hLEC junction integrity and reduced paracellular transport. Our study highlights the effect of fibroblasts on lymphatic functions during homeostasis, critical to understanding potential mechanistic targets that could allow lymphatic functions to return to homeostasis during disease.

RESULTS

Exposure to fibroblast secretomes modulates lymphatic cell-cell junctions and reduces lymphatic permeability.

To understand the effect of fibroblasts on hLEC junction, we first optimized the media conditions for fibroblast secretome collection. We found that the characteristic morphology and growth pattern of NHDF cells were similar in endothelial microvascular growth media (EGMV2), as this media also contains fibroblast growth factors. NHDFs were grown in fibroblast growth media (FGM) with 1ng/ml of fibroblast growth factor and 5 µg/ml of insulin - NHDF (G), or in basal FGM - NHDF(B). Then, NHDFs were exposed to EGMV2 media for 2 days and NHDF secretome was collected. hLECs were grown in a monolayer on transwell insert and then treated with NHDF (G) or (B) secretomes for 2 days (**Figure 1A**). We first assessed hLEC barrier integrity using transendothelial electrical resistance (TEER). Treatment with NHDF(G) and NHDF(B) secretomes resulted in significantly higher TEER values of 85 ± 8 Ω-cm^2 and 57 ± 12 Ω-cm^2, respectively, compared to 37 ± 8 Ω-cm^2 for the controls (**Figure 1B**). Next, we sought to analyze hLEC cell-cell junction integrity and expression via immunofluorescence. We found that tight junction proteins ZO-1 and claudin-5 and adherens junction protein VE-cadherin expression significantly increased with both the NHDF secretomes compared to controls (**Figure 1C&D**). Specifically, treatment with NHDF(G) led to 4-, 3-, and 4-fold increases in the expression levels of VE-cadherin, claudin-5, and ZO-1, while NHDF(B) treatment resulted in 4-, 2-, and 5-fold upregulation of the junction proteins, respectively (**Figure 1D**). We also found that lymphatic endothelial markers, LYVE-1 and PROX1, were not altered (**Figure 1E & Supplementary figure 1A**). To evaluate changes in hLEC monolayer permeability following treatment with fibroblast secretomes, we assessed transport of a fluorescently labeled, 4kDa dextran (FD4). We observed a reduction in permeability, decreasing by 24% from 11 ± 1% in the control group to 8 ± 1% with NHDF(G) secretome treated group after 8-hours (**Figure 1F**).

Co-culture with fibroblasts regulates LEC junction expression and reduces lymphatic permeability

To address the direct effects of fibroblasts on the lymphatic junction expression and permeability, we generated a non-contact co-culture model (**Figure 2A**), where hLECs are cultured on the bottom of the transwell and after monolayers were established, NHDFs are seeded on the transwell top. Cells were co-cultured 2 days (**Figure 2B**), after which fibroblasts were scraped from the membrane to prevent interference with TEER and permeability measurements. hLEC monolayers exhibited increased TEER values after co-culture with NHDF

(G) and (B), rising from 46 ± 13 for the control group to 112 ± 5 with NHDF(G) and 95 ± 15 with NHDF(B) treatments (**Figure 2C**). We also found a distinct increase in ZO-1 and VE-cadherin expression in both co-culture groups (**Figure 2D**). VE-cadherin expression increased by 1.6- and 1.3-fold, while ZO-1 expression increased by 2.1- and 2.0-fold in the NHDF(G) and NHDF(B) groups, respectively, compared to the control group (**Figure 2E**). FD4 permeability across the hLEC monolayer decreased by 30% following co-culture with NHDF(G), and by 15% with NHDF(B), indicating reduced permeability(**Figure 2F)**.

We performed detailed analysis of LEC junction morphology using the Junction Analyzer Program (JAnaP) [17], a Python-based program that quantitatively analyzes cell-cell junction presentation along with the cell morphology. We found no difference in the cellular solidity, but did see an 18% decrease in the cell circularity in hLECs co-cultured with NHDF(G) (**Figure 3A**). Both NHDF(G) and -(B) promote lymphatic monolayers, increasing hLEC coverage by 7%. We also found a significant increase in ZO-1 continuous junctions from 84 ± 5% in controls to 96 ± 2% in both co-cultures. Similarly, both co-cultures significantly reduced ZO1 discontinuous junctions, with a reduction in punctate junctions by 89% and 97% and perpendicular junctions by 64% and 62% with NHDF(G) and NHDF (B), respectively (**Figure 3A**). Immunoblot analysis showed no notable increase in overall ZO-1 (220 kDa) and VE-cadherin (120 kDa) protein levels compared to the control (**Figure 3B**). Similarly, mRNA expression levels of ZO-1 and VE-cadherin did not differ significantly from the control (**Figure 3C**).

Fibroblasts show tissue-specific effects on lymphatic junctions and permeability.

To investigate tissue specific effects of fibroblasts on lymphatic functions, we exposed hLECs to secretome from normal human lung fibroblasts (NHLF). While found a significant increase in junction integrity and TEER with dermal fibroblast (NHDF) secretomes, we detected the opposite trend with NHLFs. We found a significant decrease in TEER from 87 ± 5 Ω-cm^2 in control to 72 ± 2 Ω-cm^2 with NHLF secretomes (**Figure 4A**). Immunofluorescence imaging revealed an 18% reduction in ZO-1 expression following treatment with NHLF secretome, compared to the control while treatment with NHLF media left expression unchanged. (**Figure 4B&C**). We found no significant change in VE-cadherin expression compared to control. Consistent with the reduction in TEER and ZO1 expression, we observed a 2-fold increase in FD4 transport across hLECs treated with NHLF secretome compared to controls. We also saw that this effect was dose-dependent, as the FD4 transport increases with an increase in secretome proportion (**Figure 4D**).

Fibroblasts promote thrombin-induced LEC barrier dysfunction

Thrombin, a potent inflammatory mediator is known to induce vascular dysfunction and increase endothelial permeability in blood vasculature. However, the effects of thrombin signaling on lymphatic function, particularly its impact on permeability, remain to be fully understood. Studies on HUVECs have shown that thrombin disrupts endothelial integrity by altering VE-cadherin and catenin interactions [18]. We examined the impact thrombin on hLECs in the presence of fibroblasts. hLECs were exposed to thrombin for 4 hours or left untreated, followed by a 48-hour co-culture with NHDF, with an hLEC-only group serving as a control. Thrombin treatment caused a reduction in TEER values in hLECs by 19%, while a 12% decrease was observed in the NHDF co-culture group (**Figure 5A**). Thrombin treatment also led to a reduction in hLEC numbers for both control and NHDF groups, suggesting a potential impact on cell viability or proliferation (**Figure 5B**). Additionally, we assessed the permeability of hLECs to FD4 after thrombin treatment in response to NHDF co-culture. Consistent with the TEER findings, thrombin increased dextran transport by 30% in hLECs in the presence of fibroblasts (**Figure 5C**). Immunofluorescence analysis of junction proteins in thrombin-treated hLECs showed an irregular junction protein expression between the cell-cell monolayer. When hLECs were co-cultured with NHDF after thrombin treatment, they exhibited noticeably larger junction discontinuity (**Figure 5D**).

DISCUSSION

The main objective of this study was to assess how fibroblasts regulate lymphatic permeability and barrier function. Our findings indicate that fibroblasts play a pivotal role as paracrine regulators in maintaining homeostasis by enhancing LEC junction integrity and reducing permeability in dermal lymphatic vessels. We demonstrate that the dermal fibroblast secretomes decrease lymphatic junction permeability by enhancing tight and adherens junction proteins. Our data suggests that secretome treatment increases junction integrity, as evidenced by increased TEER across LEC monolayers treated with secretomes dermal fibroblast cultures. Fibroblast secretomes increased the expression of key junctional proteins, ZO-1, claudin-5, and VE-cadherin on hLEC surface to regulate junction morphology and paracellular transport, compared to untreated controls. We also found that treating LECs with dermal fibroblast secretomes markedly reduced transport of a small, 4 kDa dextran. Finally, we found that these effects appeared to be tissue specific, as lung fibroblasts had opposite effects on hLEC integrity compared to dermal fibroblasts.

We observed that high expression of junction proteins is related to the integrity of endothelial cells monolayer. This is corroborated by others, as who previously demonstrated that junction localization of claudin-5 is essential for maintaining the integrity of collecting lymphatic vessels. This process is regulated by the signaling of the transmembrane ligand EphrinB2 and its receptor EphB4 [19]. Using proximity proteomics, Serafin et al. revealed changes in the VE-cadherin interactome during the transition from discontinuous to continuous LEC junctions, observing complete overlap of VE-cadherin expression in continuous cell-cell junctions [2]. Additionally, Cromer et al. investigated the regulation of lymphatic barrier function by inflammatory cytokines, showing that inflammatory signals increase LEC permeability by reducing VE-cadherin expression [20]. Jannaway and Scallan showed a 5.7-fold increase in 3-kDa dextran transport while blocking VE-cadherin, suggesting its critical role in maintaining lymphatic barrier functions [1]. Our data also indicated a similar effect, where increased expression of VE-cadherin and ZO-1 was associated with reduced dextran transport across the monolayer. Apart from junction proteins, secretome treatment did not significantly affect LEC-specific markers such as LYVE-1 and PROX1. This suggests that LEC markers are constitutively expressed and not significantly modulated during homeostasis.

Our co-culture data corroborated the findings from secretome-treated LECs, demonstrating that fibroblasts promote continuous presentation of ZO-1 and VE-cadherin, and reducing transport. However, lymphatic permeability is not always directly associated with changes in LEC junctional proteins. For example, a study using rat LECs reported an increase in LEC permeability and TEER induced by ethanol, despite no changes in ZO-1 or VE-cadherin expression or localization [21]. We observed similar results when examining the overall expression of junction proteins using immunoblotting and RT-qPCR analyses, which revealed no significant difference in the overall protein and mRNA expression of ZO-1 and VE-cadherin. This suggests that fibroblasts may not directly influence the translation of ZO-1 and VE-cadherin but could instead be promoting their trafficking and organization at cell-cell boundaries. Recently, Dellaquila et al, showed that HUVECs co-cultured with neonatal foreskin fibroblasts had 50% reduced permeability to 70 kDa dextrans [22]. Another study co-culturing HUVECs and lung fibroblasts showed a drop in dextran permeability for HUVECs from 61% to 39% after 7 days and to 7% after two weeks [23]. Consistent with these findings, our results also show a significant reduction in lymphatic permeability upon co-culture with dermal fibroblasts. This suggests that fibroblasts may promote remodeling of LECs towards collecting vessel phenotypes. However, further studies are needed to investigate the transition of lymphatic capillaries towards collecting vessels in presence of fibroblast.

Notably, LECs were treated with secretome or introduced with fibroblasts after forming a complete LEC monolayer, highlighting the dynamic and homeostatic regulatory effect of fibroblasts on mature LECs. This is important as most of the previous studies demonstrated the role of fibroblasts in regulating LEC proliferation, lymphangiogenesis, and tube/branch formation. For instance, fibroblast-like cells have been shown to regulate the population of total endothelial cells within lymph nodes, including LECs, through paracrine signaling, primarily by secreting VEGF, which promotes cell proliferation [24]. In an in vivo study, Goto and colleagues demonstrated that interactions between LECs and surrounding fibroblasts facilitate epithelial regeneration in the small intestine [25]. Wang et al. further identified the role of specific fibroblast populations in VEGF-C-mediated lymphangiogenesis in zebrafish [10]. Additionally, Marino et al. reported that dermal fibroblasts induced lymphatic capillary branching in LECs, but only under direct contact conditions, with no branching observed when using fibroblast secretomes or a non-contact transwell setup [26]. Most of the studies discussed suggested a direct role of fibroblast in maintaining lymphatic development and vascularization. In our studies, we also see a positive correlation between hLEC coverage and the presence of fibroblast. However, the effect of fibroblast in regulating LEC integrity suggests fibroblast could be one of the key players in maintaining collecting vessels' low permeability and preventing leakage in homeostasis in the skin.

Fibroblasts are known to play role in different tissue environment. Our data so far suggest the effect of dermal fibroblasts on maintaining dermal LEC integrity. However, unlike with the dermal fibroblasts, we found that lung fibroblast secretomes reduced TEER and increased FD4 transport across LEC monolayers, indicating more leaky junctions and a corresponding decline in LEC junction integrity. Surprisingly, the effect of NHLF on hLECs are opposite to what we observed with NHDF. This indicates that fibroblasts regulate LEC permeability differently depending on the tissue environment. Lung fibroblasts interact with various immune cells, influencing the severity and outcomes of many acute and chronic lung diseases, while dermal fibroblasts are key components of connective tissue, playing a role in ECM formation and wound healing. Studies have shown that dermal and pulmonary fibroblasts respond differently to TGF-β1 and PDGF-AB, highlighting the heterogeneity of fibroblasts across different tissues [27]. Lung LECs also differ significantly from dermal LECs. Lung lymphatics are directly involved in clearing airborne toxins, gas exchange, and immune response regulation, whereas dermal LECs maintain a regular fluid homeostasis and immune surveillance within the skin layer. Lung lymphatics also lack smooth muscle coverage unlike other collecting lymphatics and rely on extrinsic muscle contraction of breathing. In this study, we have also found a contrary effects of

lung and dermal fibroblasts on LECs permeability that might indicate tissue specific regulation of LEC functions by fibroblasts.

Since lymphatic vessels play a key role in clearing proinflammatory mediators and immune cells to resolve inflammation, we aimed to investigate the direct impact of the inflammatory mediator thrombin on LECs in the presence of fibroblasts. A recent study reported that both human blood endothelial cells and fibroblasts can generate thrombin without the need for exogenous protein addition [28]. Previous research on dermal LECs demonstrated that thrombin reduces TEER, while pretreatment with 8-Br-cAMP mitigated this effect [29]. Additionally, researchers identified proinflammatory mediators, including thrombin, as contributors to lymphatic capillary regression [30]. Trivedi et al. used RNA sequencing of lung LECs isolated from cigarette smoke-exposed mice, revealing an upregulation of inflammatory mediators and prothrombotic pathways. Their findings further confirmed that cigarette smoke-induced lung dysfunction is associated with increased thrombin levels [31]. While some studies suggest that thrombin compromises the lymphatic barrier, we observed minimal changes in LEC junctions upon thrombin treatment alone. However, in the presence of fibroblasts, we detected significant alterations in TEER and permeability, as indicated by increased dextran transport. Moreover, thrombin-treated LECs co-cultured with fibroblasts exhibited large gaps in the monolayer compared to control LECs. These findings suggest that fibroblasts not only influence the permeability of lymphatic endothelial junctions but also modulate the effects of other mediators on LECs.

Taken together, our work explores the influence of biological and physiological factors modulating LEC barrier functions in their local microenvironment. LECs are surrounded by and influenced by stromal cells and immune cells, and we demonstrate that fibroblasts play a key role in maintaining lymphtic homeostasis. Our study demonstrated that dermal fibroblasts primarily enhance LEC integrity by promoting high expression of tight and adherens proteins at cell junctions, which plays a critical role in controlling paracellular transport. Thus, fibroblasts modulate lymphatic barrier function by affecting cell-cell junctional interaction. However, the effect of fibroblasts on LECs showed heterogeneity and tissue specificity which warrants further investigations.

MATERIALS AND METHODS

Cell culture and co-culture model

Human primary dermal lymphatic endothelial cells (hLECs) (PromoCell, C-12217) were seeded onto the bottom side of Transwell inserts (1 µm pore size, Falcon®, 353103), coated with 50 µg/mL rat tail collagen I (Corning, 354236). After seeding hLECs for 1 hour at 37 °C, inserts were turned around and cells allowed to grow for 5 days in Endothelial Cell Growth Medium MV2 (EGM-V2; PromoCell, C-22121) until the hLECs formed a confluent monolayer. Monolayer formation was confirmed by measurement of transendothelial resistance (TEER) or by staining with CellMask™ Plasma Membrane Stain (ThermoFisher, C10046).

Normal human primary dermal fibroblasts (NHDF) were cultured in two conditions: (1) NHDF(G) (PromoCell, C-12302) in Fibroblast Growth Medium-2 (PromoCell, C-23120) containing 2% FBS, 1 ng/mL fibroblast growth factor, and 5 µg/mL insulin, or (2) NHDF(B) in fibroblast basal medium without supplements. For secretome collection, fibroblasts were cultured with EGM2 for 24 hours. Media was then collected and centrifuged to remove debris, and the resulting conditioned medium (secretome) was used for treatment. Normal human primary lung fibroblasts (NHLF; Lonza, CC-2512) were cultured in FGM-2 (Lonza, CC-3132) and processed similarly to NHDFs for secretome collection. The hLEC monolayers on inserts were treated at the top side with either (1) NHDF cells (NHDF(G) or NHDF(B)) or (2) their corresponding secretomes, for 48 hours. Following co-culture, secretomes were removed, and fibroblasts were either detached using a sterile cotton applicator (Dealmed, B074MJHSGG) or left untreated. hLECs were then processed for other assays. For thrombin experiments, 2 U/mL thrombin was added to the hLEC monolayer at the top. After treatment, inserts were washed thoroughly, and hLECs were co-cultured with NHDF(G) cells for 48 hours prior to downstream analysis.

Transendothelial electrical resistance (TEER)

To assess the confluence and barrier integrity of hLEC monolayers TEER was measured using a Millicell® ERS-2 Voltohmmeter (Millipore). Electrodes were carefully positioned in both the upper and lower chambers of the Transwell system, ensuring contact with the culture medium. Initial resistance values (in ohms) were recorded and corrected by subtracting background resistance values obtained from blank inserts (without cells). Final TEER values ($\Omega \cdot cm^2$) were calculated by multiplying the resistance of the cell-containing inserts by the surface area of the 12-well Transwell membrane (1.12 cm^2). These measurements were used to confirm monolayer confluency and LEC barrier integrity prior to downstream assays.

In vitro lymphatic transport assay

To evaluate the effect of fibroblasts or their secretomes on LEC permeability, hLEC monolayers were subjected to a transport assay following co-culture or treatment [32]. After removing fibroblasts or secretomes, hLECs were washed and incubated with fresh EGMV2 basal media. Media containing 20 µg/mL FITC-labeled dextran 4 kDa (FD4; Millipore Sigma, 46944) was added to the upper chamber of the Transwell insert. The transport assay was carried out for 8 hours at 37 °C. At defined timepoints, aliquots were collected from the lower chamber (plate bottom), and fluorescence intensity was measured using a microplate reader (Tecan Spark) and standard curve. The amount of FD4 transported across the hLEC monolayer was used as a quantitative readout of lymphatic permeability.

Immunofluorescence staining, confocal microscopy and imaging analyses

For immunofluorescence imaging and downstream analysis, hLECs were fixed in 2% paraformaldehyde (PFA) in 1X phosphate-buffered saline (PBS; Thermo Fisher, J19943.K2) for 15 minutes at room temperature, then permeabilized with 0.1% Triton X-100. Cells were blocked in 2% fetal bovine serum (FBS; Gibco, 10100-147) in PBS for 1 hour. Membranes were carefully excised and mounted onto glass slides. Cells were incubated overnight at 4°C with primary antibodies: mouse anti-VE-cadherin (1:200; BD Biosciences, 55566) and rabbit anti-ZO-1 (1:200; Invitrogen, 33-9100). The following day, cells were incubated with species-specific Alexa Fluor-conjugated secondary antibodies—donkey anti-mouse Alexa Fluor 488, 555, or 647 (1:400; Invitrogen, A21202, A31570 or A31571) and donkey anti-rabbit Alexa Fluor 488, 555, or 647 (1:400; Invitrogen, A32790, 31572 and A31573)—for 2 hours at room temperature. Washes were performed with 0.1% Tween-20 in 1X PBS (BioShop, TWN510) before and after antibody incubations. Nuclei were counterstained using Hoechst 33342 (1:10,000) and cover slips were mounted using VECTAshield Antifade Mounting Medium with DAPI (Vector Laboratories, H-1200-10). Images were acquired using a Zeiss Observer 7 fluorescence microscope (20X/63X objectives) or an FV3000 laser scanning confocal microscope (20X/100X objectives).

Immunoblot assay and qPCR

After co-culture, hLECs were lysed using RIPA lysis buffer (Thermo Fisher, 89900). The resulting cell lysates were subjected to gel electrophoresis and immunoblotting as previously described [33]. Briefly, 20 µg of protein per lane was denatured in Laemmli buffer and separated on a 4–20% SDS-PAGE gel (Mini-Protein TGX, BioRad) at 110V for 1 hour. Proteins were then transferred to nitrocellulose membranes (Trans-Blot Turbo, BioRad) using a semi-dry transfer

system (1.5 mA, 25 V for 7 minutes), and membrane transfer was confirmed via Ponceau S staining. The membranes were sectioned into strips, blocked in 2% BSA (prepared in TBS-T) for 1 hour, and incubated overnight at 4°C with primary antibodies: mouse anti-VE-cadherin (BD Biosciences, 55566) and rabbit anti-ZO-1 (Invitrogen, 33-9100) at a 1:500 dilution. After washing, the membranes were incubated for 1 hour at room temperature with secondary antibodies: IRDye® 680RD donkey anti-Rabbit, donkey anti-Mouse, and IRDye® 800CW donkey anti-Rabbit (all at 1:20,000 dilution). Protein bands were visualized using the Odyssey® Imaging System (LI-COR).

To quantify expression of genes encoding adherens and tight junction proteins, total RNA was isolated from hLEC samples using TRIzol™ reagent (Invitrogen, 15596026), following the manufacturer's protocol. To obtain sufficient RNA for analysis, biological replicates were generated by pooling RNA extracted from four individual transwell inserts. A total of 500 ng of RNA per sample was reverse transcribed into cDNA using the High-Capacity cDNA Reverse Transcription Kit (Applied Biosystems, 4374966), according to the manufacturer's instructions. Quantitative real-time PCR (RT-qPCR) was performed using TaqMan™ Gene Expression Assays specific for VE-cadherin (CDH5, Hs00901465), ZO-1 (TJP1, Hs01551871), PROX1 (Hs00896293), LYVE-1 (Hs00272659), and the housekeeping gene GAPDH (Hs02786624). Relative gene expression levels of hLECs after co-culture were calculated using the comparative Ct method (ΔΔCt) and relative fold changes ($2^{-\Delta\Delta Ct}$) were determined with respect to control.

Image Processing

Image analysis, including cell counts and quantification of mean fluorescence intensity for junction proteins, was conducted using FIJI (ImageJ2, version 2.14). For detailed single-cell analysis, the Junction Analyzer Program (JANaP) was utilized, as previously described [17]. Junction morphology of hLECs was classified as either continuous (linear or mature) or discontinuous, which included isolated, jagged, punctate, or perpendicular junctional patterns. In addition, cell shape descriptors such as circularity and solidity were quantified to assess morphological changes.

Statistical Analysis

All analysis was performed using GraphPad software (version 10.4.2), and data are represented as mean ± standard error of the mean (SEM). Statistical analysis was performed using an unpaired two-tailed *t*-test; $p > 0.05$ = not significant (ns), $p \leq 0.0001$ = extremely significant

(****). For the permeability (transport) assay, statistical significance was determined by two-way ANOVA followed by appropriate post hoc test for multiple comparisons.

ACKNOWLEDGMENTS:

This work was supported by financial support from NIGMS MIRA 1R35GM142835-01 (KM). We would also like to thank the UMD Bioworkshop core facility for support and use of confocal microscopy.

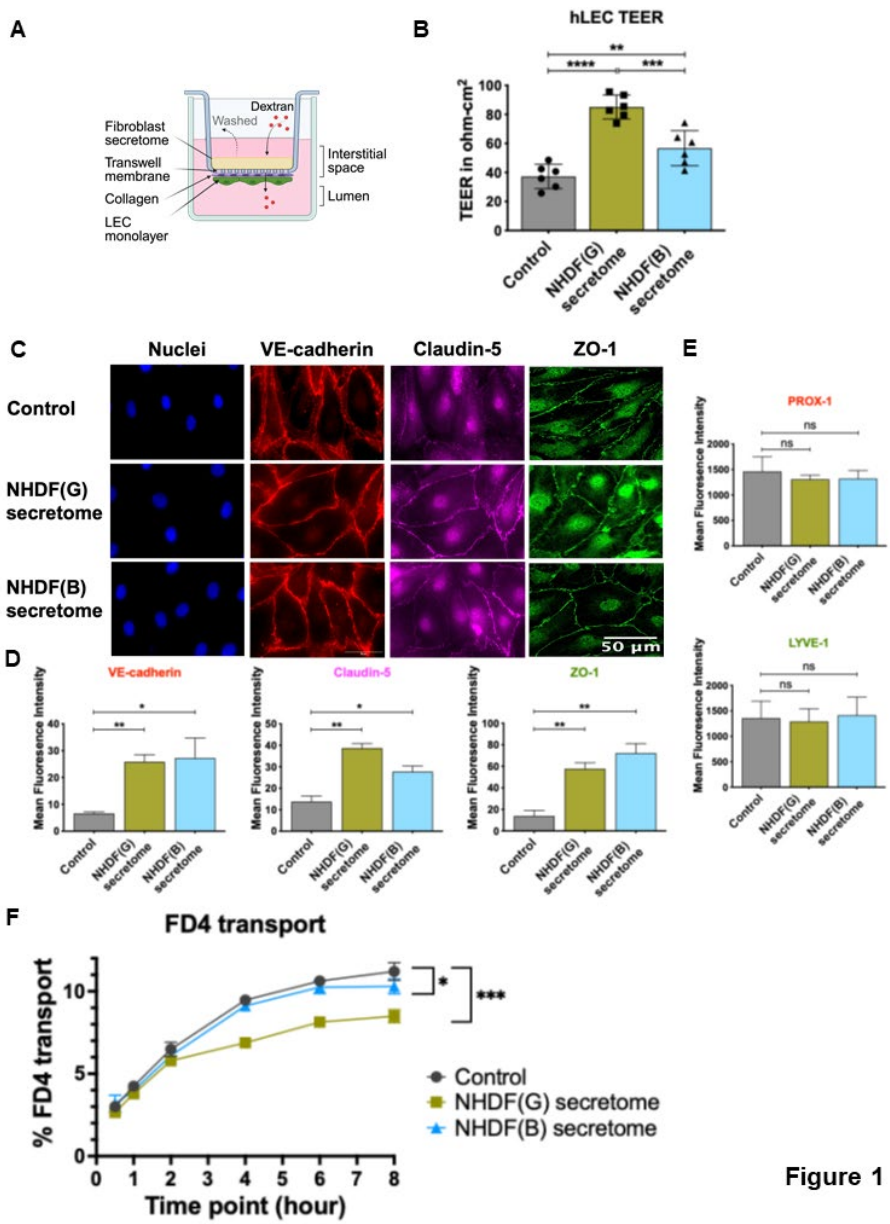

Figure 1. ***NHDF secretomes increase hLEC barrier functions.*** **(A)** Schematic diagram of transwell secretome experiment. (**B)** TEER measurements of hLEC monolayers after 48 hours of treatment with dermal fibroblast secretomes with [NHDF(G)] and without growth factors [NHDF(B)]. (**C)** Representative immunofluorescence images of VE-cadherin, claudin-5, and ZO-1 on hLECs following treatment with NHDF secretomes. **(D)** Quantification of VE-cadherin, claudin-5, and ZO-1 expression levels using ImageJ (FIJI). **(E)** Quantification of lymphatic markers LYVE-1 and PROX1 expression in hLEC monolayers treated with NHDF secretomes. **(F)** FITC–Dextran (4 kDa) transport assay across hLECs after NHDF secretome treatment. Data are presented as mean ± SEM from n = 6 independent experiments. Statistical analysis was performed using an unpaired two-tailed t-test; $p > 0.05$ = not significant (ns), $p \leq 0.0001$ = extremely significant (****). For the permeability (transport) assay (n = 3, representative), statistical significance was determined by two-way ANOVA followed by appropriate post hoc test for multiple comparisons.

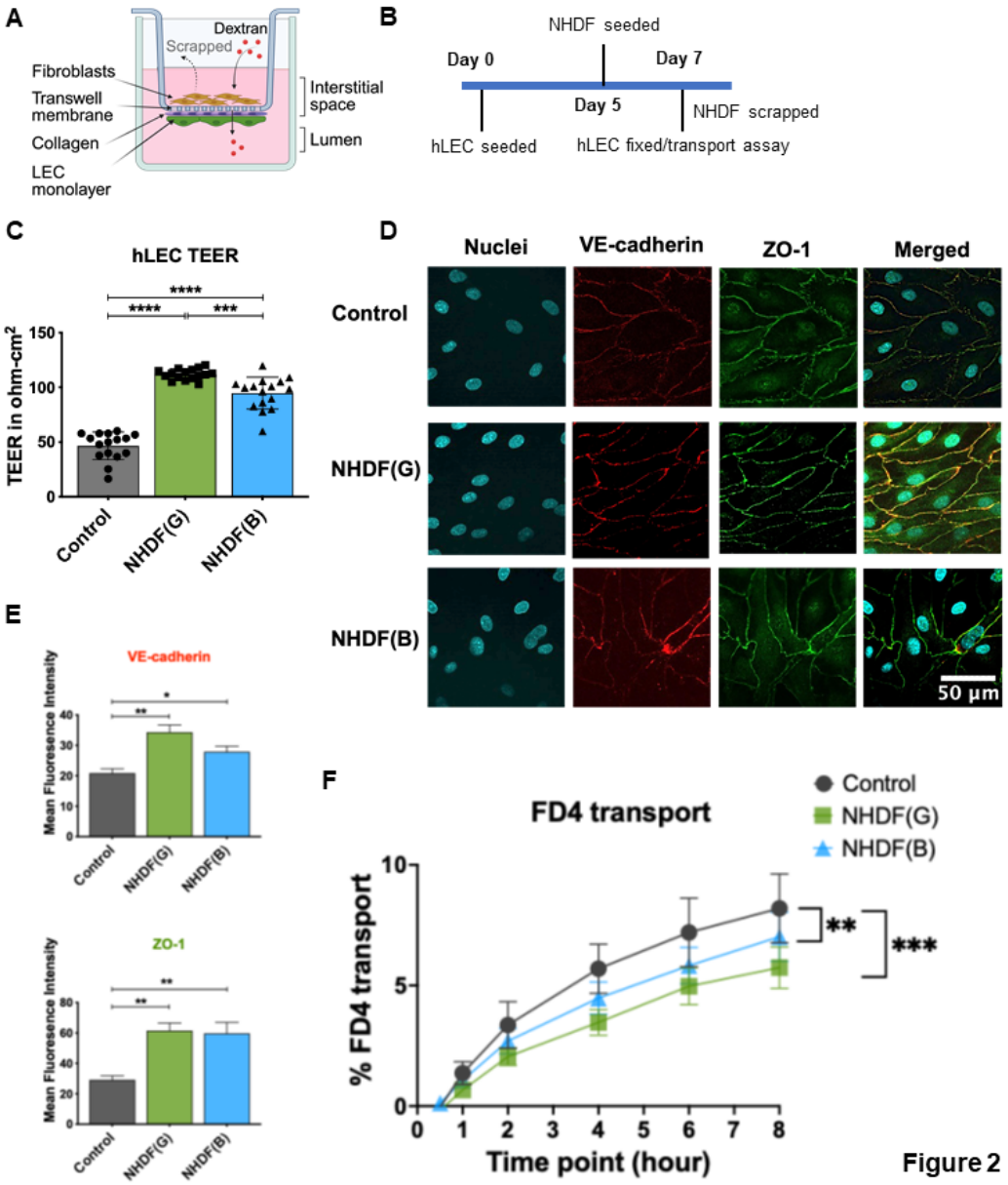

Figure 2. ***NHDF co-culture with hLECs increases hLEC barrier functions.*** **(A)** Schematic diagram of transwell co-culture experiment. **(B)** Schematic diagram of cells seedings and co-culture. **(C)** TEER measurements of hLEC monolayers after 48 hours of co-culture with dermal fibroblast with [NHDF(G)] and without growth factors [NHDF(B)]. **(D)** Representative immunofluorescence images of VE-cadherin, and ZO-1 on hLECs following co-culture with NHDFs. **(E)** Quantification of VE-cadherin and ZO-1 expression levels using ImageJ (FIJI). **(F)** FITC–Dextran (4 kDa) transport assay across hLECs after co-culture with NHDFs. Data are presented as mean ± SEM from n = 6 independent experiments. Statistical analysis was performed using an unpaired two-tailed t-test; $p > 0.05$ = not significant (ns), $p \leq 0.0001$ = extremely significant (****). For the permeability (transport) assay (n = 5, representative), statistical significance was determined by two-way ANOVA followed by appropriate post hoc test for multiple comparisons.

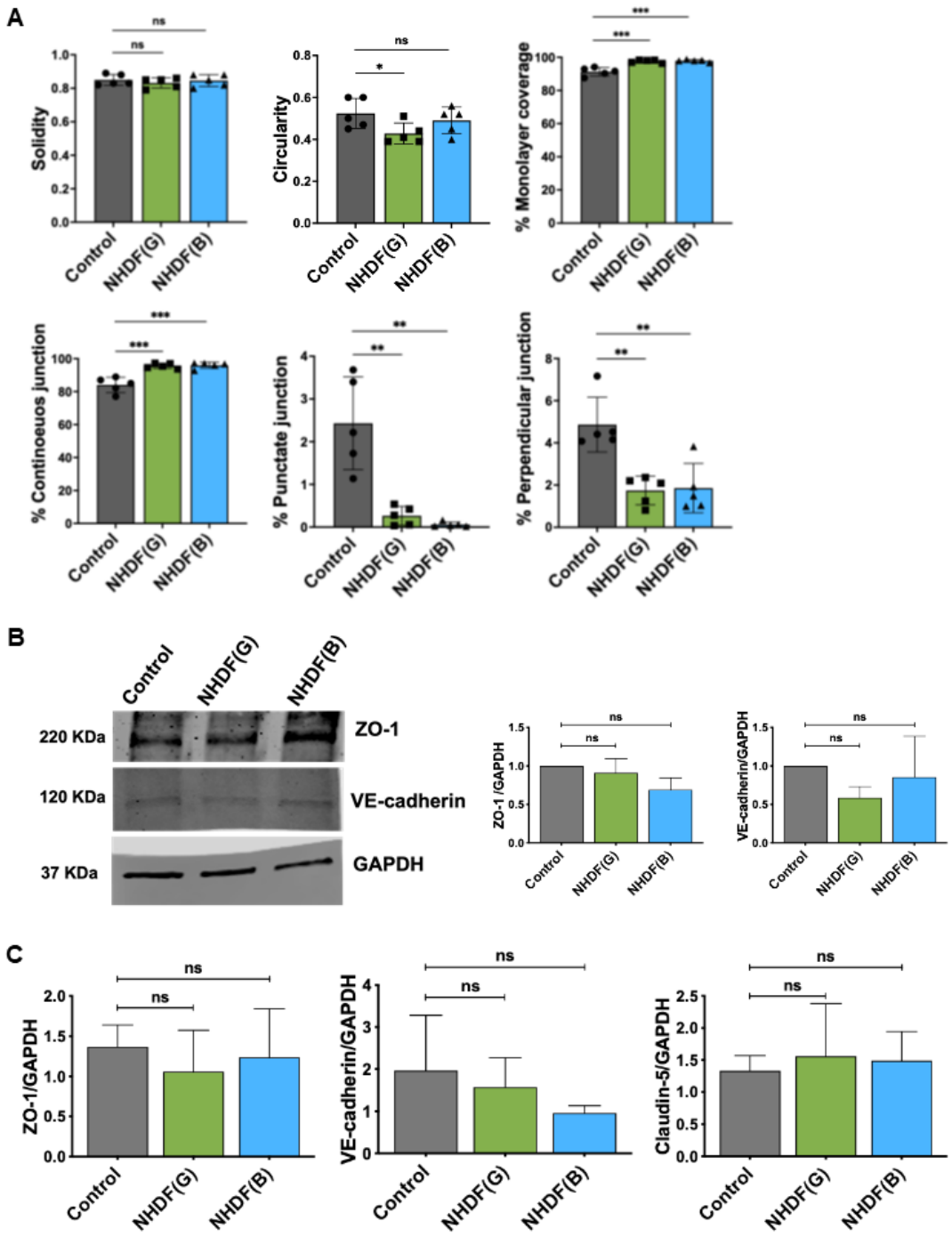

Figure 3. ***hLEC junctions are tightened after co-culture with NHDFs.*** **(A)** Quantitative analysis of ZO-1 distribution and organization in hLEC monolayers using JAnaP after 48 hours of co-culture with NHDFs. **(B)** Immunoblot analysis of total ZO-1 (220 kDa) and VE-cadherin (120 kDa) protein expression levels in hLECs following co-culture. **(C)** RT-qPCR analysis of mRNA expression levels of ZO-1 and VE-cadherin in hLECs under the same conditions. Data are presented as mean ± SEM from $n > 2$ independent experiments. Statistical analysis was performed using an unpaired two-tailed *t*-test; $p > 0.05$ = not significant (ns), $p \leq 0.0001$ = extremely significant (****).

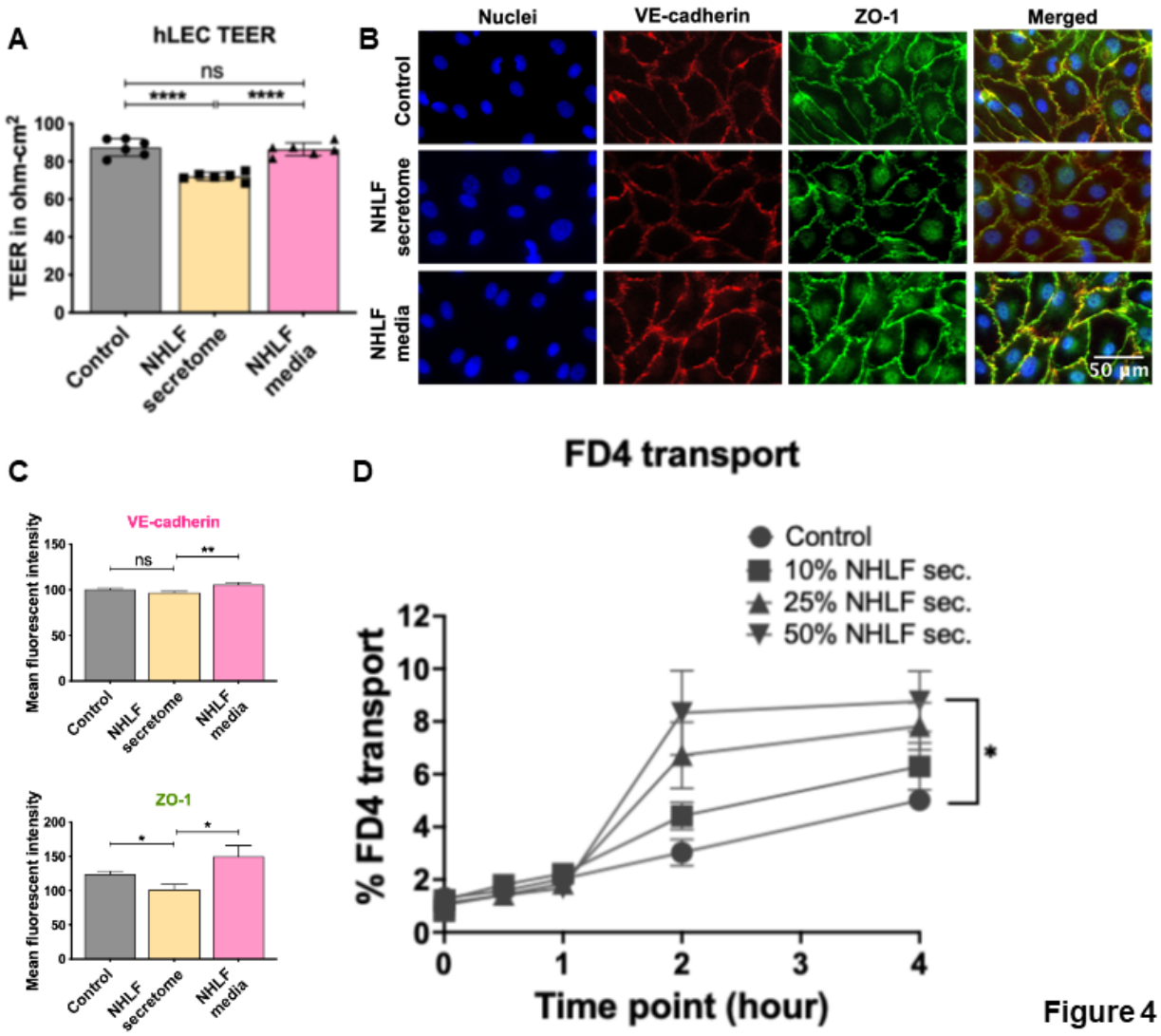

Figure 4. ***NHLF secretomes reduce hLEC barrier functions.*** **(A)** TEER measurements of hLEC monolayers after 48 hours of treatment with NHLF secretomes or fibroblast media. **(B)** Representative immunofluorescence images of VE-cadherin, and ZO-1 on hLECs following treatment with NHLF secretome. **(C)** Quantification of VE-cadherin and ZO-1 expression levels using ImageJ (FIJI). **(D)** FITC–Dextran (4 kDa) transport assay across hLECs after treatment with 10, 25 and 50% NHLF secretome. Data are presented as mean ± SEM from $n = 6$ independent experiments. Statistical analysis was performed using an unpaired two-tailed *t*-test; $p > 0.05$ = not significant (ns), $p \leq 0.0001$ = extremely significant (****). For the transport assay ($n = 3$, representative), statistical significance was determined by two-way ANOVA followed by appropriate post hoc test for multiple comparisons.

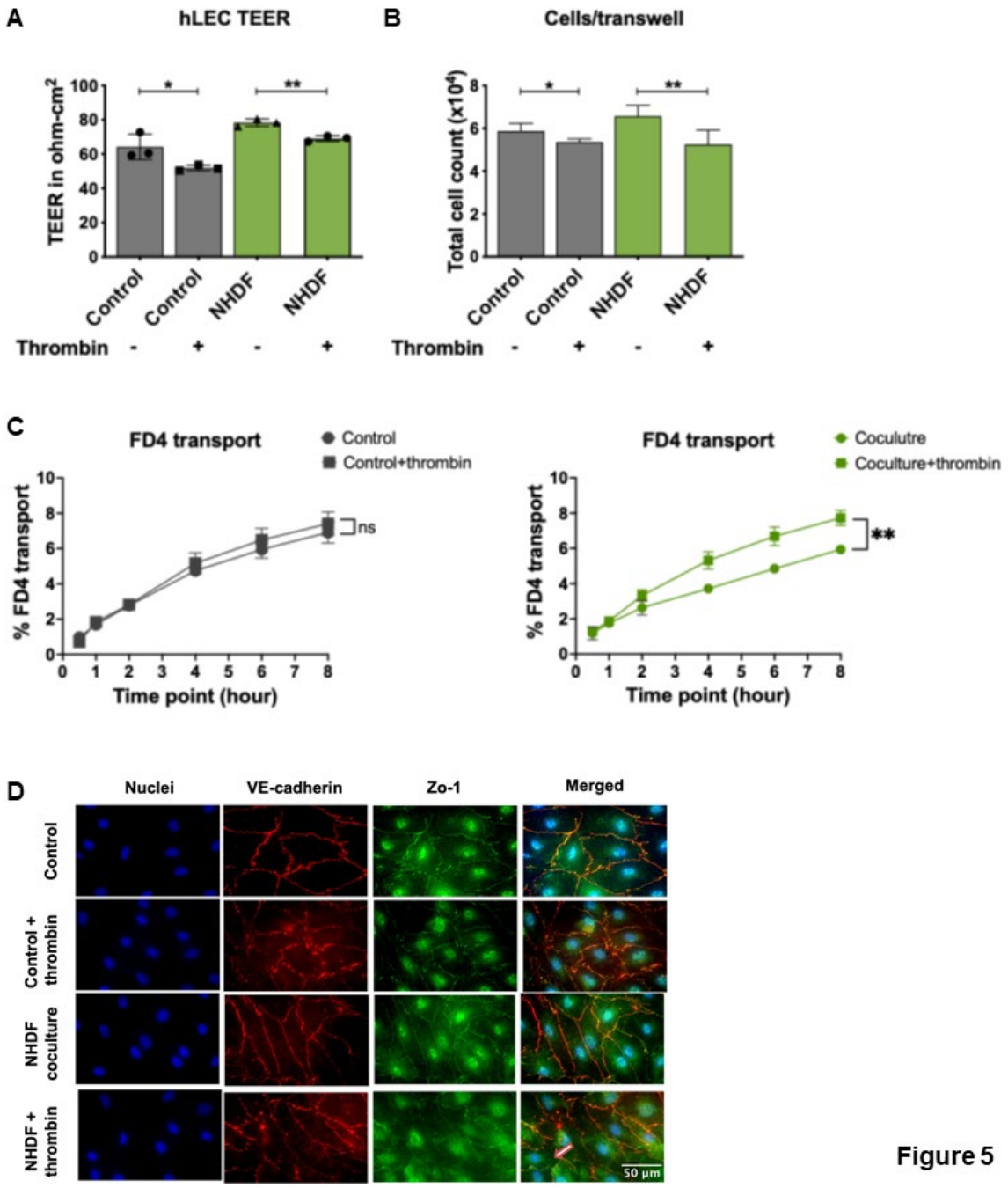

Figure 5. ***Thrombin modulates hLEC barrier integrity only in the context of co-culture with NHDFs***. **(A)** TEER measurements of hLEC monolayers after 4 hours of thrombin treatment followed by 48 hours of co-culture with dermal fibroblast (NHDF(G) (*n* = *3*). **(B)** Total cell counts (*n* = *6*). **(C)** FITC–Dextran (4 kDa) transport assay across hLECs after 4 hours of thrombin stimulation and/or NHDF co-culture for 48 hours. **(D)** Representative immunofluorescence images of ZO-1 and VE-cadherin on hLECs with and without thrombin treatment. Data are presented as mean ± SEM from *n* = *3-6* independent experiments. Statistical analysis was performed using an unpaired two-tailed *t*-test; $p > 0.05$ = not significant (ns), $p \leq 0.0001$ = extremely significant (****). For the transport assay, statistical significance was determined by two-way ANOVA followed by appropriate post hoc test for multiple comparisons.

References

1. Jannaway, M., & Scallan, J. P. (2021). VE-Cadherin and Vesicles Differentially Regulate Lymphatic Vascular Permeability to Solutes of Various Sizes. Frontiers in physiology, 12, 687563. https://doi.org/10.3389/fphys.2021.687563

2. Serafin, D. S., Harris, N. R., Bálint, L., Douglas, E. S., & Caron, K. M. (2024). Proximity interactome of lymphatic VE-cadherin reveals mechanisms of junctional remodeling and reelin secretion. *Nature communications*, *15*(1), 7734. https://doi.org/10.1038/s41467-024-51918-1

3. Peluzzo, A. M., Bkhache, M., Do, L. N. H., Autieri, M. V., & Liu, X. (2023). Differential regulation of lymphatic junctional morphology and the potential effects on cardiovascular diseases. Frontiers in physiology, 14, 1198052. https://doi.org/10.3389/fphys.2023.1198052

3. Kajiya, K., Kidoya, H., Sawane, M., Matsumoto-Okazaki, Y., Yamanishi, H., Furuse, M., & Takakura, N. (2012). Promotion of lymphatic integrity by angiopoietin-1/Tie2 signaling during inflammation. The American journal of pathology, 180(3), 1273–1282. https://doi.org/10.1016/j.ajpath.2011.11.008

5. Miteva, D. O., Rutkowski, J. M., Dixon, J. B., Kilarski, W., Shields, J. D., & Swartz, M. A. (2010). Transmural flow modulates cell and fluid transport functions of lymphatic endothelium. *Circulation research*, *106*(5), 920–931. https://doi.org/10.1161/CIRCRESAHA.109.207274

6. Ilan, I. S., Yslas, A. R., Peng, Y., Lu, R., & Lee, E. (2023). A 3D Human Lymphatic Vessel-on-Chip Reveals the Roles of Interstitial Flow and VEGF-A/C for Lymphatic Sprouting and Discontinuous Junction Formation. *Cellular and molecular bioengineering*, *16*(4), 325–339. https://doi.org/10.1007/s12195-023-00780-0

7. Frye, M., Taddei, A., Dierkes, C., Martinez-Corral, I., Fielden, M., Ortsäter, H., Kazenwadel, J., Calado, D. P., Ostergaard, P., Salminen, M., He, L., Harvey, N. L., Kiefer, F., & Mäkinen, T. (2018). Matrix stiffness controls lymphatic vessel formation through regulation of a GATA2-dependent transcriptional program. Nature communications, 9(1), 1511.

8. Norden, P. R., & Kume, T. (2021). Molecular Mechanisms Controlling Lymphatic Endothelial Junction Integrity. *Frontiers in cell and developmental biology*, *8*, 627647. https://doi.org/10.3389/fcell.2020.627647

9. Hong, S. P., Yang, M. J., Cho, H., Park, I., Bae, H., Choe, K., Suh, S. H., Adams, R. H., Alitalo, K., Lim, D., & Koh, G. Y. (2020). Distinct fibroblast subsets regulate lacteal integrity through YAP/TAZ-induced VEGF-C in intestinal villi. *Nature communications*, *11*(1), 4102. https://doi.org/10.1038/s41467-020-17886-y

10. Wang, G., Muhl, L., Padberg, Y., Dupont, L., Peterson-Maduro, J., Stehling, M., le Noble, F., Colige, A., Betsholtz, C., Schulte-Merker, S., & van Impel, A. (2020). Specific fibroblast subpopulations and neuronal structures provide local sources of Vegfc-processing components during zebrafish lymphangiogenesis. *Nature communications*, *11*(1), 2724. https://doi.org/10.1038/s41467-020-16552-7

11. Karkkainen, M. J., Haiko, P., Sainio, K., Partanen, J., Taipale, J., Petrova, T. V., Jeltsch, M., Jackson, D. G., Talikka, M., Rauvala, H., Betsholtz, C., & Alitalo, K. (2004). Vascular endothelial growth factor C is required for sprouting of the first lymphatic vessels from embryonic veins. Nature immunology, 5(1), 74–80. https://doi.org/10.1038/ni1013

12. Lee, E., Chan, S. L., Lee, Y., Polacheck, W. J., Kwak, S., Wen, A., Nguyen, D. T., Kutys, M. L., Alimperti, S., Kolarzyk, A. M., Kwak, T. J., Eyckmans, J., Bielenberg, D. R., Chen, H., & Chen, C. S. (2023). A 3D biomimetic model of lymphatics reveals cell-cell junction tightening and lymphedema via a cytokine-induced ROCK2/JAM-A complex. Proceedings of the National Academy of Sciences of the United States of America, 120(41), e2308941120. https://doi.org/10.1073/pnas.2308941120

13. Yu, P., Wilhelm, K., Dubrac, A., Tung, J. K., Alves, T. C., Fang, J. S., Xie, Y., Zhu, J., Chen, Z., De Smet, F., Zhang, J., Jin, S. W., Sun, L., Sun, H., Kibbey, R. G., Hirschi, K. K., Hay, N., Carmeliet, P., Chittenden, T. W., Eichmann, A., … Simons, M. (2017). FGF-dependent metabolic control of vascular development. Nature, 545(7653), 224–228. https://doi.org/10.1038/nature22322

14. Wei, W. F., Zhou, H. L., Chen, P. Y., Huang, X. L., Huang, L., Liang, L. J., Guo, C. H., Zhou, C. F., Yu, L., Fan, L. S., & Wang, W. (2023). Cancer-associated fibroblast-derived PAI-1 promotes lymphatic metastasis via the induction of EndoMT in lymphatic endothelial cells. Journal of experimental & clinical cancer research : CR, 42(1), 160. https://doi.org/10.1186/s13046-023-02714-0

15. Lugo-Cintrón, K. M., Ayuso, J. M., Humayun, M., Gong, M. M., Kerr, S. C., Ponik, S. M., Harari, P. M., Virumbrales-Muñoz, M., & Beebe, D. J. (2021). Primary head and neck

tumour-derived fibroblasts promote lymphangiogenesis in a lymphatic organotypic co-culture model. *EBioMedicine*, *73*, 103634. https://doi.org/10.1016/j.ebiom.2021.103634

16. Chiu, A., Jia, W., Sun, Y., Goldman, J., & Zhao, F. (2023). Fibroblast-Generated Extracellular Matrix Guides Anastomosis during Wound Healing in an Engineered Lymphatic Skin Flap. *Bioengineering (Basel, Switzerland)*, *10*(2), 149. https://doi.org/10.3390/bioengineering10020149

17. Gray, K. M., Katz, D. B., Brown, E. G., & Stroka, K. M. (2019). Quantitative Phenotyping of Cell-Cell Junctions to Evaluate ZO-1 Presentation in Brain Endothelial Cells. *Annals of biomedical engineering*, *47*(7), 1675–1687. https://doi.org/10.1007/s10439-019-02266-5

18. Rabiet, M. J., Plantier, J. L., Rival, Y., Genoux, Y., Lampugnani, M. G., & Dejana, E. (1996). Thrombin-induced increase in endothelial permeability is associated with changes in cell-to-cell junction organization. *Arteriosclerosis, thrombosis, and vascular biology*, *16*(3), 488–496. https://doi.org/10.1161/01.atv.16.3.488

19. Frye, M., Stritt, S., Ortsäter, H., Hernandez Vasquez, M., Kaakinen, M., Vicente, A., Wiseman, J., Eklund, L., Martínez-Torrecuadrada, J. L., Vestweber, D., & Mäkinen, T. (2020). EphrinB2-EphB4 signalling provides Rho-mediated homeostatic control of lymphatic endothelial cell junction integrity. eLife, 9, e57732. https://doi.org/10.7554/eLife.57732

20. Cromer, W. E., Zawieja, S. D., Tharakan, B., Childs, E. W., Newell, M. K., & Zawieja, D. C. (2014). The effects of inflammatory cytokines on lymphatic endothelial barrier function. Angiogenesis, 17(2), 395–406. https://doi.org/10.1007/s10456-013-9393-2

21. Herrera, M., Molina, P., & Souza-Smith, F. M. (2021). Ethanol-induced lymphatic endothelial cell permeability via MAP-kinase regulation. American journal of physiology. Cell physiology, 321(1), C104–C116. https://doi.org/10.1152/ajpcell.00039.2021

22. Dellaquila, A., Dujardin, C., Le Bao, C., Chaumeton, C., Carré, A., Le Guilcher, C., Lam, F., & Simon-Yarza, T. (2023). Fibroblasts mediate endothelium response to angiogenic cues in a newly developed 3D stroma engineered model. Biomaterials advances, 154, 213636. https://doi.org/10.1016/j.bioadv.2023.213636

23. Grainger, S. J., & Putnam, A. J. (2011). Assessing the permeability of engineered capillary networks in a 3D culture. PloS one, 6(7), e22086. https://doi.org/10.1371/journal.pone.0022086

24. Chyou, S., Ekland, E. H., Carpenter, A. C., Tzeng, T. C., Tian, S., Michaud, M., Madri, J. A., & Lu, T. T. (2008). Fibroblast-type reticular stromal cells regulate the lymph node vasculature. Journal of immunology (Baltimore, Md. : 1950), 181(6), 3887–3896. https://doi.org/10.4049/jimmunol.181.6.3887

25. Goto, N., Goto, S., Imada, S., Hosseini, S., Deshpande, V., & Yilmaz, Ö. H. (2022). Lymphatics and fibroblasts support intestinal stem cells in homeostasis and injury. Cell stem cell, 29(8), 1246–1261.e6. https://doi.org/10.1016/j.stem.2022.06.013

26. Marino, D., Luginbühl, J., Scola, S., Meuli, M., & Reichmann, E. (2014). Bioengineering dermo-epidermal skin grafts with blood and lymphatic capillaries. Science translational medicine, 6(221), 221ra14. https://doi.org/10.1126/scitranslmed.3006894

27. Madsen, S. F., Sand, J. M. B., Juhl, P., Karsdal, M., Thudium, C. S., Siebuhr, A. S., & Bay-Jensen, A. C. (2023). Fibroblasts are not just fibroblasts: clear differences between dermal and pulmonary fibroblasts' response to fibrotic growth factors. Scientific reports, 13(1), 9411. https://doi.org/10.1038/s41598-023-36416-6

28. Cohen, C. T., Turner, N. A., & Moake, J. L. (2021). Human endothelial cells and fibroblasts express and produce the coagulation proteins necessary for thrombin generation. *Scientific reports*, *11*(1), 21852. https://doi.org/10.1038/s41598-021-01360-w

29. Breslin J. W. (2011). ROCK and cAMP promote lymphatic endothelial cell barrier integrity and modulate histamine and thrombin-induced barrier dysfunction. *Lymphatic research and biology*, *9*(1), 3–11. https://doi.org/10.1089/lrb.2010.0016

30. Kemp, S. S., Penn, M. R., Koller, G. M., Griffin, C. T., & Davis, G. E. (2022). Proinflammatory mediators, TNFα, IFNγ, and thrombin, directly induce lymphatic capillary tube regression. *Frontiers in cell and developmental biology*, *10*, 937982. https://doi.org/10.3389/fcell.2022.937982

31. Trivedi, A., Lu, T. M., Summers, B., Kim, K., Rhee, A. J., Houghton, S., Byers, D. E., Lis, R., & Reed, H. O. (2024). Lung lymphatic endothelial cells undergo inflammatory and prothrombotic changes in a model of chronic obstructive pulmonary disease. *Frontiers in cell and developmental biology*, *12*, 1344070. https://doi.org/10.3389/fcell.2024.1344070

32. McCright, J., Skeen, C., Yarmovsky, J., & Maisel, K. (2022). Nanoparticles with dense poly(ethylene glycol) coatings with near neutral charge are maximally transported across

lymphatics and to the lymph nodes. *Acta biomaterialia*, *145*, 146–158. https://doi.org/10.1016/j.actbio.2022.03.054

33. Ejazi, S. A., Bhattacharyya, A., Choudhury, S. T., Ghosh, S., Sabur, A., Pandey, K., Das, V. N. R., Das, P., Rahaman, M., Goswami, R. P., & Ali, N. (2018). Immunoproteomic Identification and Characterization of Leishmania Membrane Proteins as Non-Invasive Diagnostic Candidates for Clinical Visceral Leishmaniasis. *Scientific reports*, *8*(1), 12110. https://doi.org/10.1038/s41598-018-30546-y